

As a library, NLM provides access to scientific literature. Inclusion in an NLM database does not imply endorsement of, or agreement with, the contents by NLM or the National Institutes of Health.

Learn more: [PMC Disclaimer](#) | [PMC Copyright Notice](#)

## Author Manuscript

Peer reviewed and accepted for publication by a journal



[J Bone Miner Res](#). Author manuscript; available in PMC: 2014 Aug 1.

Published in final edited form as: [J Bone Miner Res](#). 2013 Apr;28(4):875–885. doi: [10.1002/jbmr.1814](#)

# Partial Reductions in Mechanical Loading Yield Proportional Changes in Bone Density, Bone Architecture, and Muscle Mass

[Rachel Ellman](#)<sup>1,2</sup>, [Jordan Spatz](#)<sup>1,2,3</sup>, [Alison Cloutier](#)<sup>2</sup>, [Rupert Palme](#)<sup>4</sup>, [Blaine A Christiansen](#)<sup>2,5</sup>, [Mary L Bouxsein](#)<sup>2,3</sup>

[Author information](#) [Copyright and License information](#)

PMCID: PMC4118556 NIHMSID: NIHMS604860 PMID: [23165526](#)

The publisher's version of this article is available at [J Bone Miner Res](#)

## Abstract

Although the musculoskeletal system is known to be sensitive to changes in its mechanical environment, the relationship between functional adaptation and below-normal mechanical stimuli is not well defined. We investigated bone and muscle adaptation to a range of reduced loading using the partial weight suspension (PWS) system, in which a two-point harness is used to offload a tunable amount of body weight while maintaining quadrupedal locomotion. Skeletally mature female C57Bl/6 mice were exposed to partial weight bearing at 20%, 40%, 70%, or 100% of body weight for 21 days. A hindlimb unloaded (HLU) group was included for comparison in addition to age-matched controls in normal housing. Gait kinematics was measured across the full range of weight bearing, and some minor alterations in gait from PWS were identified. With PWS, bone and muscle changes were generally proportional to the degree of unloading. Specifically, total body and hindlimb bone mineral density, calf muscle mass, trabecular bone volume of the

distal femur, and cortical area of the femur midshaft were all linearly related to the degree of unloading. Even a load reduction to 70% of normal weight bearing was associated with significant bone deterioration and muscle atrophy. Weight bearing at 20% did not lead to better bone outcomes than HLU despite less muscle atrophy and presumably greater mechanical stimulus, requiring further investigation. These data confirm that the PWS model is highly effective in applying controllable, reduced, long-term loading that produces predictable, discrete adaptive changes in muscle and bone of the hindlimb.

**Keywords:** MECHANICAL LOADING, DISUSE, MECHANOSTAT, FUNCTIONAL ADAPTATION, WEIGHT BEARING

## Introduction

---

According to Frost's mechanostat theory,<sup>(1,2)</sup> bone adapts its structure to maintain the strain engendered by physiological loading within a threshold range. Studies using animal models of overloading (mechanical loading above the threshold range) have allowed further refinement to the mechanostat theory by describing the dependence of bone formation on mechanical parameters such as strain rate, strain frequency, strain magnitude, loading history, daily strain stimulus, and rest insertion.<sup>(3)</sup> Animal studies have also been used to investigate musculoskeletal adaptation to underloading (loading below the threshold range) using complete unloading of the hindlimbs via tail suspension,<sup>(4)</sup> denervation,<sup>(5)</sup> tendon resection,<sup>(6)</sup> cast immobilization,<sup>(7)</sup> and muscle paralysis via botulinum toxin A.<sup>(8)</sup> However, the musculoskeletal responses to lesser degrees of unloading are still ill defined for lack of a suitable animal model. Thus, fundamental questions regarding the rate, extent, and distribution of disuse-induced bone loss and their dependence on a particular mechanical stimulus level are as yet unanswered. Delineating the relationships between mechanical stimuli and skeletal responses along this unloading continuum is crucial for mitigating deleterious skeletal effects of reduced weight bearing associated with clinical conditions such as muscular dystrophy, cerebral palsy, and stroke. Additionally, understanding this association can aid in assessing the risks of musculoskeletal atrophy and injury resulting from space exploration in partial gravity environments.<sup>(9)</sup>

To address this gap in knowledge, our group previously developed the partial weight suspension (PWS) system<sup>(10)</sup> that enables long-term exposure of mice to partial loading while maintaining quadrupedal locomotion. We previously implemented this model for one loading condition, 38% weight bearing, and reported bone and muscle atrophy that was less for this partial weight bearing (PWB) condition than prior studies employing tail suspension.<sup>(10)</sup> However, this work did not explore a range of partial loading levels or compare outcomes directly to a traditional model of unloading, namely hindlimb unloading (HLU) via tail suspension. Additionally, gait characterization was incomplete, because only gait kinetics was measured without assessing how PWB might affect gait kinematics. Thus, the overall goal of this study was to employ the PWS model to further explore musculoskeletal adaptation along the continuum of loading between disuse and normal weight bearing. Our primary question was whether variable PWB differentially influences muscle atrophy and bone loss. In particular, we hypothesized there would be a linear relationship between the extent of weight

bearing and the degree of bone and muscle loss. In addition, we further characterized the PWS model by studying gait kinematics, systemic stress, and the effect of the harnessing apparatus itself on bone and muscle outcomes.

## Subjects and Methods

---

### Overview of study design

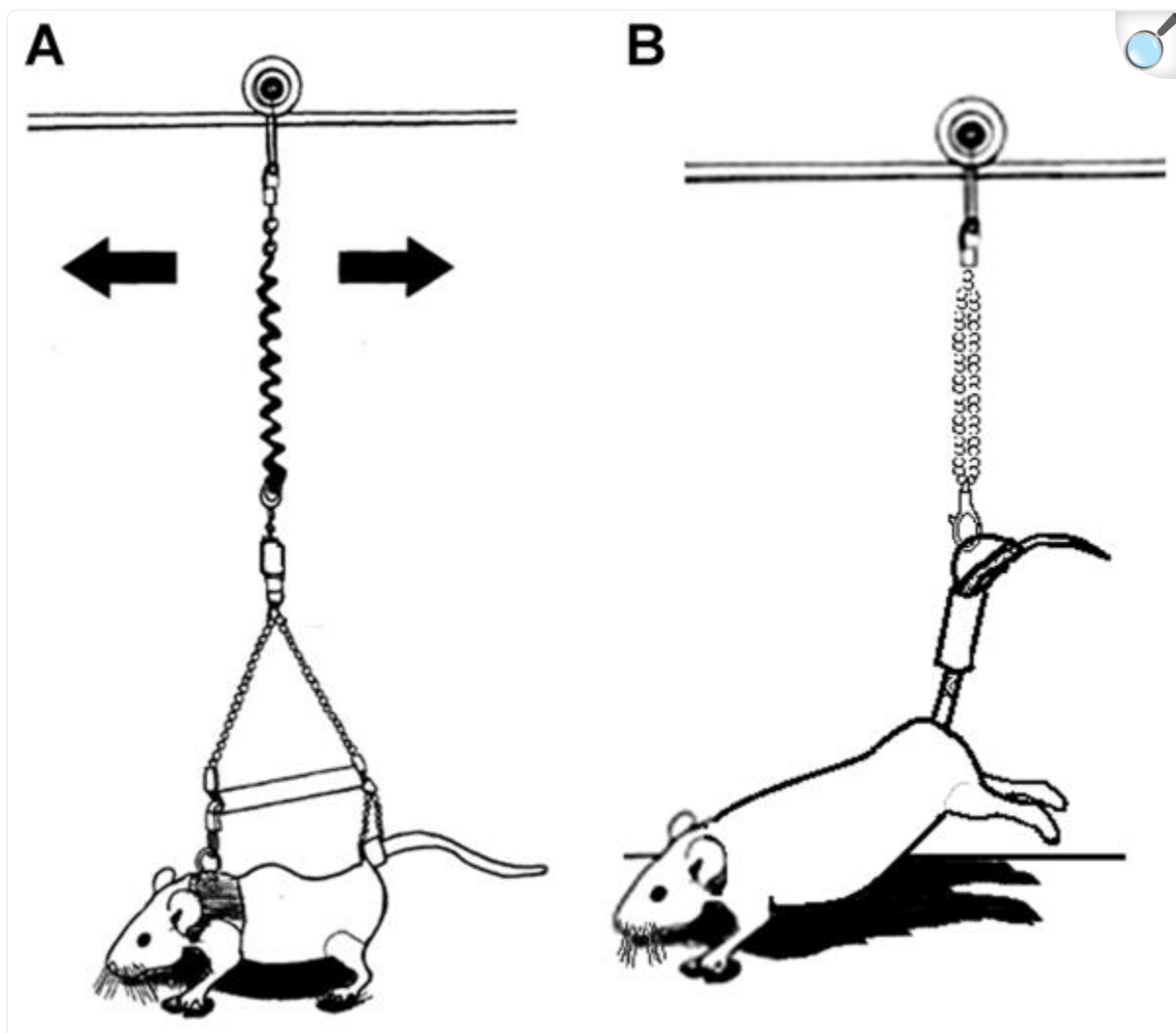
We exposed adult mice to 21 days of PWB at 20%, 40% and 70% of body weight, or total HLU and measured bone and muscle adaptation using dual-energy X-ray absorptiometry (DXA), micro-computed tomography ( $\mu$ CT), mechanical testing, and muscle mass measurements. Two additional fully loaded groups, one harnessed at 100% weight bearing and another in standard vivarium cages, were included as controls. Separately, we measured gait kinematics at PWB levels of 20%, 40%, 60%, and 80% to characterize any adjustments to walking in the PWS system. The protocol was approved by the Beth Israel Deaconess Medical Center Institutional Animal Care and Use Committee.

### Loading models

#### PWB

Two to 3 days prior to suspension, mice in the PWB groups were placed in a forelimb vest and singly housed in standard vivarium cages for acclimation. On day 0, mice were placed in a two-point PWS rig ([Fig. 1A](#)), as described.<sup>(10)</sup> Briefly, the harness was connected to the mouse in two locations, using a tape wrap at the tail base and a hook on the dorsum of the forelimb vest, and attached through a spring to a wheel with linear freedom along a rail across the top of a cage. The same custom 12-inch-cube cages were used for both PWB and HLU groups. Adjustments to actual weight bearing, or effective mass, were made by threading the spring through its support, thereby changing the length of the spring. Effective mass was measured during stationary standing while harnessed over a scale.

Fig. 1.



[Open in a new tab](#)

(A) Partial weight-bearing harness maintains the mouse in a quadrupedal orientation while partially offloading body weight using a spring connected to a support rod via a wheel. Reproduced from J Appl Physiol. 2010;109:350–7. (B) Hindlimb unloading harness suspends the mouse by the tail to prevent the hind paws from touching the ground.

## HLU

HLU animals were suspended by their tail for total unloading of the hindlimbs ([Fig. 1B](#)), following the recommendations of Morey-Holton and Globus.<sup>(11)</sup> Briefly, under inhaled isoflurane anesthesia, wound closure strips

were used to tape the tail to a swiveling rig hung from a wheel that ran along a rail across the top of a custom cage. The rig was adjusted such that the animal could not touch its hind paws to the floor, thereby fully unloading the hindlimbs. In the resulting roughly 30-degree head down tilt, forelimb contact with the cage floor was preserved, allowing the animal to move freely about the cage.

## Effect of PWB on gait

Gait characteristics were measured by high-speed video of the contact area of the paw while walking on a motorized transparent treadmill belt (DigiGait; Mouse Specifics, Quincy, MA, USA), as described in detail.<sup>(12)</sup> Following a period of accommodation to the harness, each 12-week-old female BALB/ C mouse ( $n=5$ ) was tested at a treadmill speed of 14 cm/s at five different weight-bearing levels (20%, 40%, 60%, 80%, and 100%) in a random order, then with the forelimb vest alone, and finally with no forelimb vest. Between each test, the mouse was given time to acclimate while walking on the treadmill for about 1 minute. Gait parameters included stride length (cm), swing width (cm), swing duration (% of total stride duration [% stride]), and stance/swing ratio for both the forelimb and hindlimb. Left and right limb measurements were averaged.

## Effect of PWB on the musculoskeletal system

### Animals and experimental design

One hundred and thirty-one skeletally mature (11 weeks old at start of unloading) female C57Bl/6J mice were obtained from Jackson Laboratories (Bar Harbor, ME, USA) and allowed to acclimatize for 1 week before being assigned by body mass to one of six groups. We subjected four groups to decreased loading: PWB at 20% of body mass (PWB20,  $n=20$ ), 40% of body mass (PWB40,  $n=21$ ) or 70% of body mass (PWB70,  $n=18$ ); or HLU via tail suspension ( $n=25$ ). We also included two control groups: a 100% weight-bearing group in the PWS harness (PWB100,  $n=10$ ) to determine the effect of the harness alone, and age-matched mice that were group-housed in standard vivarium cages (CON,  $n=37$ ). Standard rodent chow and water were provided *ad libitum*. Body mass was monitored daily for the first 5 days of suspension in HLU and PWB groups. CON mice were weighed twice per week, as were HLU mice after the initial 5 day monitoring period. Body mass measurements were continued daily for PWB groups and adjustments to spring length were made as necessary to match each animal's effective mass to the desired percentage of its body mass (ie, 20%, 40%, 70%, or 100% weight bearing). At the end of the 21-day study, mice were euthanized via carbon dioxide immersion and exsanguinated via cardiac puncture.

### Bone mineral density by DXA

Bone mineral density (BMD) of the total body (exclusive of the head) and hindlimb (from femoral neck to ankle) was

assessed by DXA (PIXImus II; GE Lunar, Madison, WI, USA) at baseline and sacrifice.

## Ex vivo muscle measurements

Upon sacrifice, the gastrocnemius and soleus muscles were dissected bilaterally and wet mass was measured. Right and left muscle masses were averaged and normalized by terminal body mass (mg/g).

## $\mu$ CT

Left femurs were dissected, cleaned of soft tissue, and wrapped in saline-soaked gauze. Samples were stored frozen at  $-20^{\circ}\text{C}$  until scanning. Cortical and trabecular bone microarchitecture of the femur were assessed according to published guidelines<sup>(13)</sup> using high-resolution  $\mu$ CT ( $\mu$ CT40; Scanco Medical, Basserdorf, Switzerland) with a 12- $\mu\text{m}$  isotropic voxel size, as described.<sup>(14)</sup> Images were acquired at 70 kVp and 114 mA, and 200 ms integration time. Two volumes were analyzed: distal metaphysis (beginning 240  $\mu\text{m}$  from the proximal end of the distal growth plate, extending 1800  $\mu\text{m}$  proximally) and midshaft (beginning at 55% of the bone length, extending 600  $\mu\text{m}$  distally). Gaussian filtration was applied to the grayscale images ( $\sigma=1$ , support =2 for distal metaphysis;  $\sigma=0.8$ , support =1 for midshaft). The trabecular and cortical bone were identified using automated algorithms and segmented using a global threshold of 247 and 672 mg hydroxyapatite (HA)/ $\text{cm}^3$ , respectively, for all scans. Morphological analyses were performed on the binarized images using direct, 3D techniques that do not rely on any assumptions about the underlying structure.<sup>(15-17)</sup> Morphometric variables of cancellous bone included bone volume fraction (Tb.BV/TV, %), trabecular thickness (Tb.Th, mm), trabecular number (Tb.N,  $\text{mm}^{-1}$ ), structure model index (SMI), and degree of anisotropy (DA). Cortical bone morphology measurements included average cortical thickness (Ct.Th, mm), total cross-sectional area (Tt.Ar,  $\text{mm}^2$ ), cortical bone area (Ct.Ar,  $\text{mm}^2$ ), cortical area fraction (Ct.Ar/Tt.Ar, %), and polar moment of inertia ( $J$ ,  $\text{mm}^4$ ).

## Mechanical testing

Left femurs were mechanically tested to failure in three-point bending. Fresh-frozen femurs were thawed to room temperature then centered longitudinally, with the anterior surface on the two lower support points spaced 10 mm apart.<sup>(18)</sup> One of two materials testing systems (MTS Bionix 200 with 100 N load cell, MTS Systems, Eden Prairie, MN, USA; Bose ElectroForce 3200 with 150 N load cell, Bose Corporation, Eden Prairie, MN, USA) was used to apply a flexion moment in the anterior-posterior plane at a constant displacement rate of 0.03 mm/s until failure. Force-displacement data were acquired at 30 Hz and used to determine maximum force (N), stiffness (N/mm), and estimated Young's Modulus (MPa).

## Effect of PWB on adrenocortical activity

Following the same experimental design for the study of the effect of PWB on the musculoskeletal system as described above, 34 mice were assigned to the HLU ( $n=5$ ), PWB20 ( $n=4$ ), PWB40 ( $n=5$ ), PWB70 ( $n=5$ ), PWB100 ( $n=5$ ), and CON ( $n=5$ ) groups. An additional control group, CON1, consisting of mice singly-housed in standard vivarium cages ( $n=5$ ) was included to test for stress induced by single housing. Feces were collected from each individual animal on day 0 (presuspension), and 1, 2, 3, 5, 8, and 10 days after suspension, except in the case of the CON group from which only one sample per time point could be acquired because of group housing. Cage flooring was cleaned 24 hours before sampling.

A  $5\alpha$ -pregnane- $3\beta$ , $11\beta$ , $21$ -triol- $20$ -one enzyme immunoassay for measuring fecal corticosterone metabolites (FCM) was used to measure adrenocortical activity, as described.<sup>(19,20)</sup> The fecal corticosterone metabolites reflect adrenocortical activity of the prior 24 hours.

## Statistical analysis

All data were checked for normality and reported as mean  $\pm$  SD, unless otherwise noted. Group differences were considered significant at  $p \leq 0.05$ . We assessed differences in gait parameters with repeated measures ANOVA separately for an effect of the harness (including 100% weight bearing, vest alone, and bare trials only) and effect of loading level (including 20%, 40%, 60%, 80%, and 100% weight-bearing trials only) stratified by limb (forelimb or hindlimb). No data were collected from 1 mouse with the vest alone due to technical difficulties. Consequently that mouse was eliminated from repeated measures analyses involving that loading condition.

For the study of effects on the musculoskeletal system, we tested for group differences in body mass, BMD, and fecal corticosterone levels at baseline among groups using one-way ANOVA. Longitudinal changes in body mass from day 0 were analyzed using repeated measures ANOVA with post hoc testing for pairwise differences. One-sample  $t$  tests were used to determine if percent changes in BMD from baseline were different from zero. To test for any differences from the control group, we compared unloaded groups to CON using ANOVA with a two-sided Dunnett's post hoc analysis. We used ANOVA to determine the effect of unloading level on ex vivo bone and muscle outcomes in the PWB20, PWB40, PWB70, and PWB100 groups, with Scheffé post hoc tests for pairwise comparisons. We used two-tailed  $t$  tests to determine whether bone and muscle outcomes differed between HLU and PWB20. To test for linear association with weight bearing we used linear regression and confirmed that the residuals were normally distributed with equal variance over the range of expected values.

Corticosterone metabolite measurements were averaged for each mouse from days 1 to 3 and from days 5 to 10, and differences among groups for each time point were determined using ANOVA with post hoc testing. Missing data for 1 PWB100 animal on day 8 was filled in by averaging the values for days 5 and 10.

## Results

---

### Effect of PWB on gait

There were no differences in gait parameters among the three 100% loading conditions (harnessed at 100% weight bearing, vest alone, no vest), except for stance width ( $p=0.03$ ), which was modified with the addition of vest alone (+30% and +6.5%) and harness (+38% and -9.5%) for the forelimbs and hindlimbs, respectively ([Table 1](#)). As expected due to the design of the forelimb jacket, stance width was more affected at the forelimbs than the hindlimbs.



Table 1.

## Gait Measurements at Different Partial Weight Bearing Conditions

	20%	40%	60%	80%	100%	Vest ( <i>n</i> =4)	No vest
Forelimb							
Stride length (cm)	3.92 ± 0.65	4.96 ± 0.33	4.56 ± 0.40	4.56 ± 0.30	4.24 ± 0.70	4.91 ± 0.40	4.16 ± 0.59
Stance width (cm)	1.96 ± 0.34	2.05 ± 0.20	2.05 ± 0.32	2.10 ± 0.19	2.14 ± 0.27	2.03 ± 0.24	1.57 ± 0.06 <sup>a, b</sup>
Swing duration (%)	38.3 ± 5.5	37.6 ± 4.3	34.7 ± 4.2	34.5 ± 5.5	31.5 ± 10.2	35.5 ± 3.8	35.6 ± 3.5
Stance/swing ratio	1.52 ± 0.26	1.70 ± 0.29	1.94 ± 0.40	1.96 ± 0.42	2.58 ± 1.25	1.85 ± 0.29	1.85 ± 0.28
Hindlimb							
Stride length (cm)	5.26 ± 1.32	5.26 ± 0.24	4.98 ± 0.29	4.90 ± 0.20	4.32 ± 1.09	5.14 ± 0.31	4.84 ± 0.71
Stance width (cm)	2.75 ± 0.37	2.69 ± 0.21	2.80 ± 0.25	2.82 ± 0.16	2.54 ± 0.15	3.00 ± 0.22	2.77 ± 0.17 <sup>a</sup>
Swing duration (%)	33.9 ± 6.3 <sup>c</sup>	29.6 ± 7.0	29.8 ± 3.5 <sup>c</sup>	27.4 ± 4.6	26.6 ± 3.3	23.9 ± 2.3	26.0 ± 3.7
Stance/swing ratio	2.01 ± 0.68 <sup>c, d</sup>	2.55 ± 0.91	2.44 ± 0.37 <sup>c</sup>	2.79 ± 0.71	2.88 ± 0.40	3.23 ± 0.39	2.90 ± 0.51

[Open in a new tab](#)

Values are mean ± SD. Post hoc test for repeated measures with no correction for multiple comparisons. Vest =with forelimb vest alone.

<sup>a</sup>Different from 100% among 100% loading conditions.

<sup>b</sup>Different from Vest among 100% loading conditions.

<sup>c</sup>Different from 100% among harnessed conditions.

<sup>d</sup>Different from 80% among harnessed conditions.

With decreased weight bearing, gait was characterized by a longer swing phase and shorter stance phase (eg, +27% and –10% at 20% PWB relative to 100% weight bearing, respectively), and a concomitant decrease in stance/swing ratio for the hindlimbs only ([Table 1](#)). There were no changes in forelimb stride time in swing and stance phases ( $p > 0.2$ ), though there was a trend toward decreased forelimb stride length with partial unloading ( $p = 0.07$ ). Stance width did differ from the 100% weight-bearing (plus harness) condition for either forelimbs or hindlimbs during PWB ( $p > 0.2$ ).

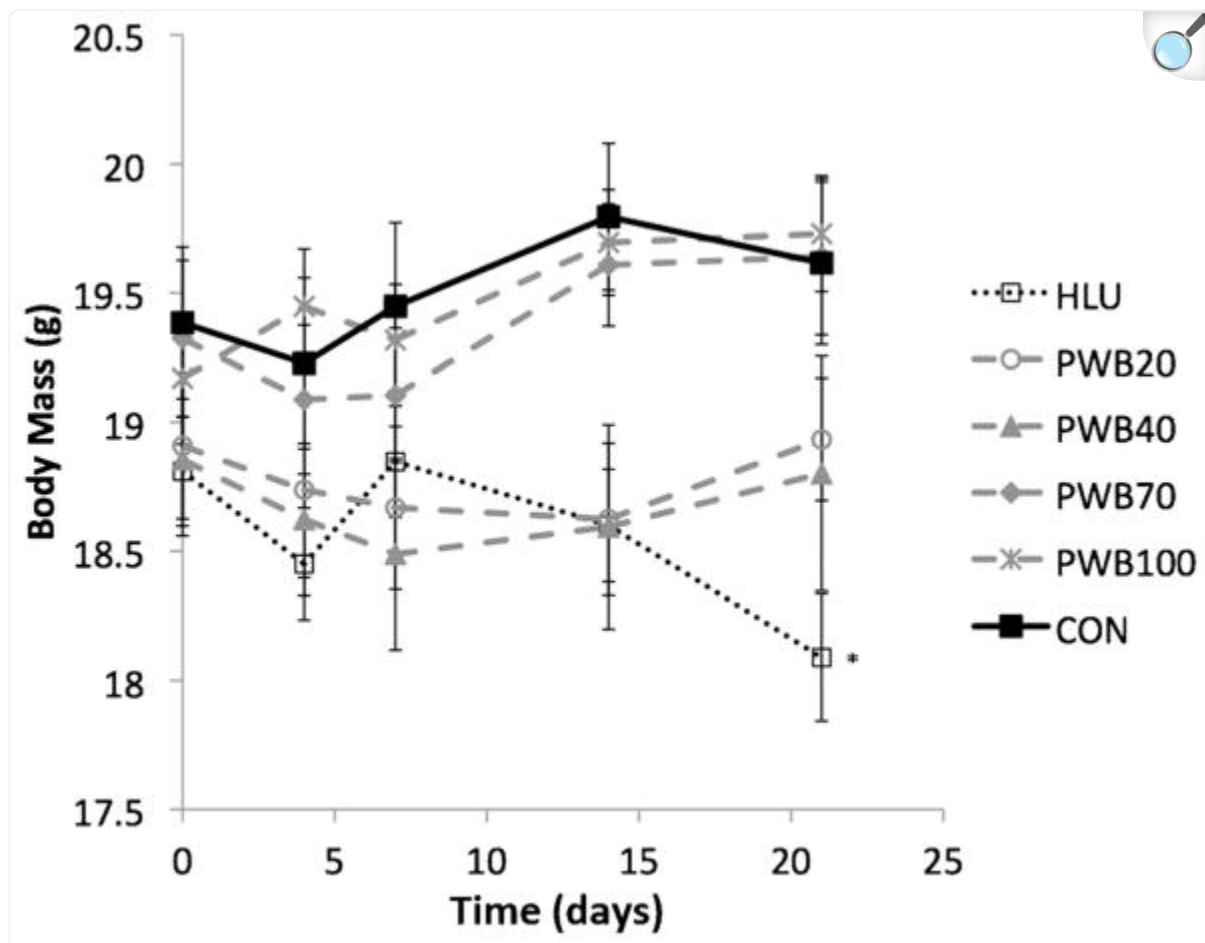
## Effects of PWB on the musculoskeletal system

The unloading interventions were generally well-tolerated. Three mice (2 HLU and 1 PWB20) were removed from the study due to excessive self-inflicted injury at the harness attachment point(s).

### Body mass

Baseline body mass ( $19.5 \pm 1.3$  g) did not differ among groups. Body mass declined slightly (less than –2%) in the HLU, PWB20, and PWB40 groups within the first 7 days ( $p < 0.05$ ; [Fig. 2](#)). By day 21, body mass returned to baseline levels in the PWB20 and PWB40 groups, but not in the HLU group (–3.7% +4.8%;  $p < 0.005$ ). The PWB70, PWB100, and CON groups gained body mass transiently during the study (+1.5% to 2.7%,  $p < 0.05$ ), but each of these groups concluded the study at their baseline body mass.

Fig. 2.



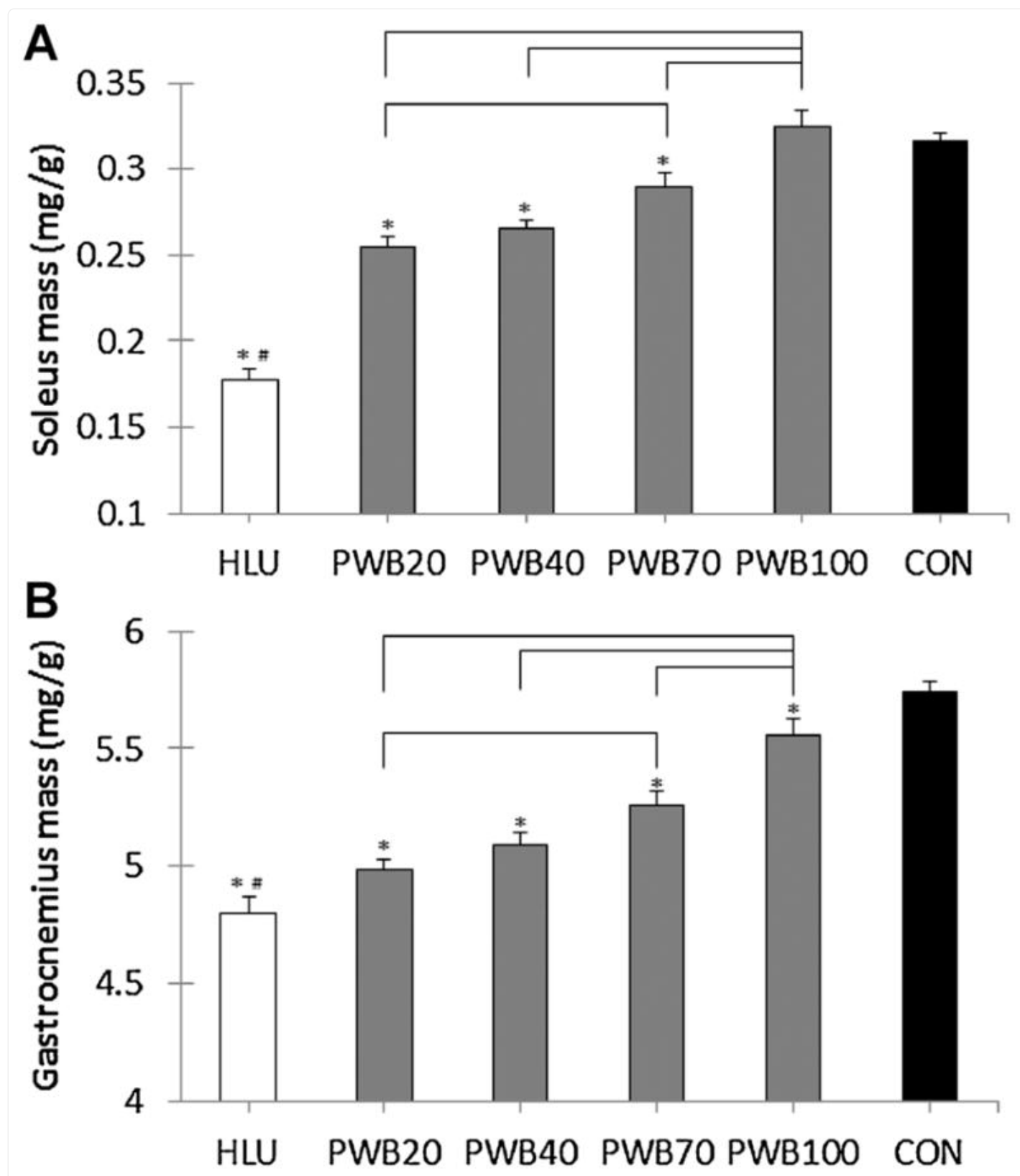
[Open in a new tab](#)

Effect of unloading intervention on body mass. Each data point represents the mean of  $\pm 2$  days  $\pm$  SEM bars. Asterisk denotes significant difference ( $p < 0.005$ ) from baseline at day 21.

## Muscle mass

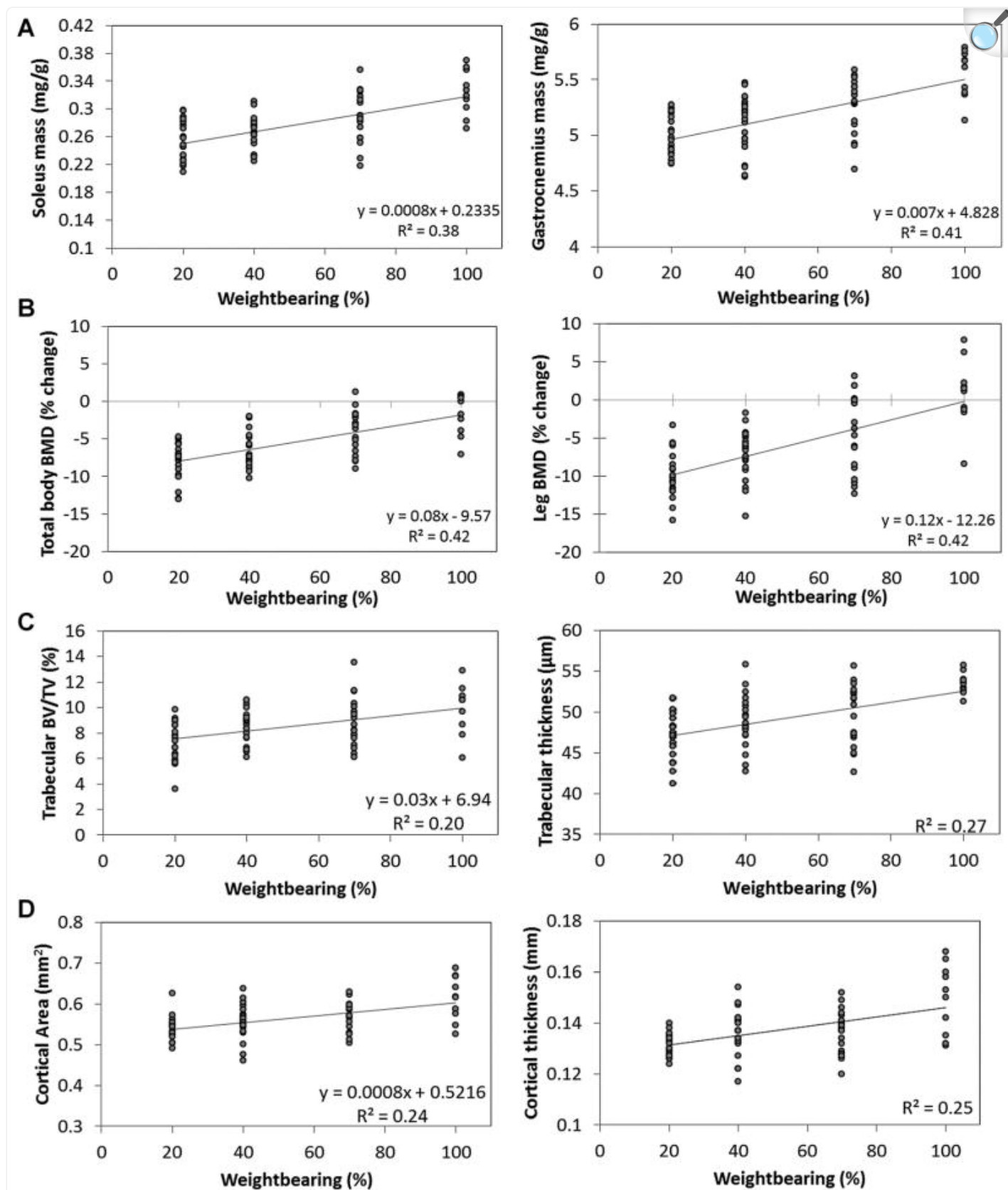
Compared to the CON and PWB100 groups, muscle weights were significantly lower in all partially unloaded groups (ie, PWB20, PWB40, PWB70;  $p < 0.05$  for all; [Fig. 3](#)). Furthermore, final soleus and gastrocnemius masses were linearly associated with weight bearing ( $p < 0.0001$ ,  $R^2 = 0.38$  and  $0.41$ , respectively; [Fig. 44](#)). Soleus and gastrocnemius muscle mass were 30% and 4% lower ( $p < 0.05$ ), respectively, in HLU than PWB20. Muscle atrophy was greater in the soleus than the gastrocnemius. For example, soleus and gastrocnemius weight were 22% and 10% lower, respectively, in PWB20 compared to PWB100.

Fig. 3.



(A) Soleus and (B) gastrocnemius wet mass normalized by body mass (mean  $\pm$ SEM). \* =Different from CON ( $p < 0.05$ ), # =HLU different from PWB20, PWB40, PWB70, and PWB100 ( $p < 0.05$ ), brackets =pairwise differences between PWB groups (ANOVA with Scheffé post hoc,  $p < 0.05$ ).

Fig. 4.



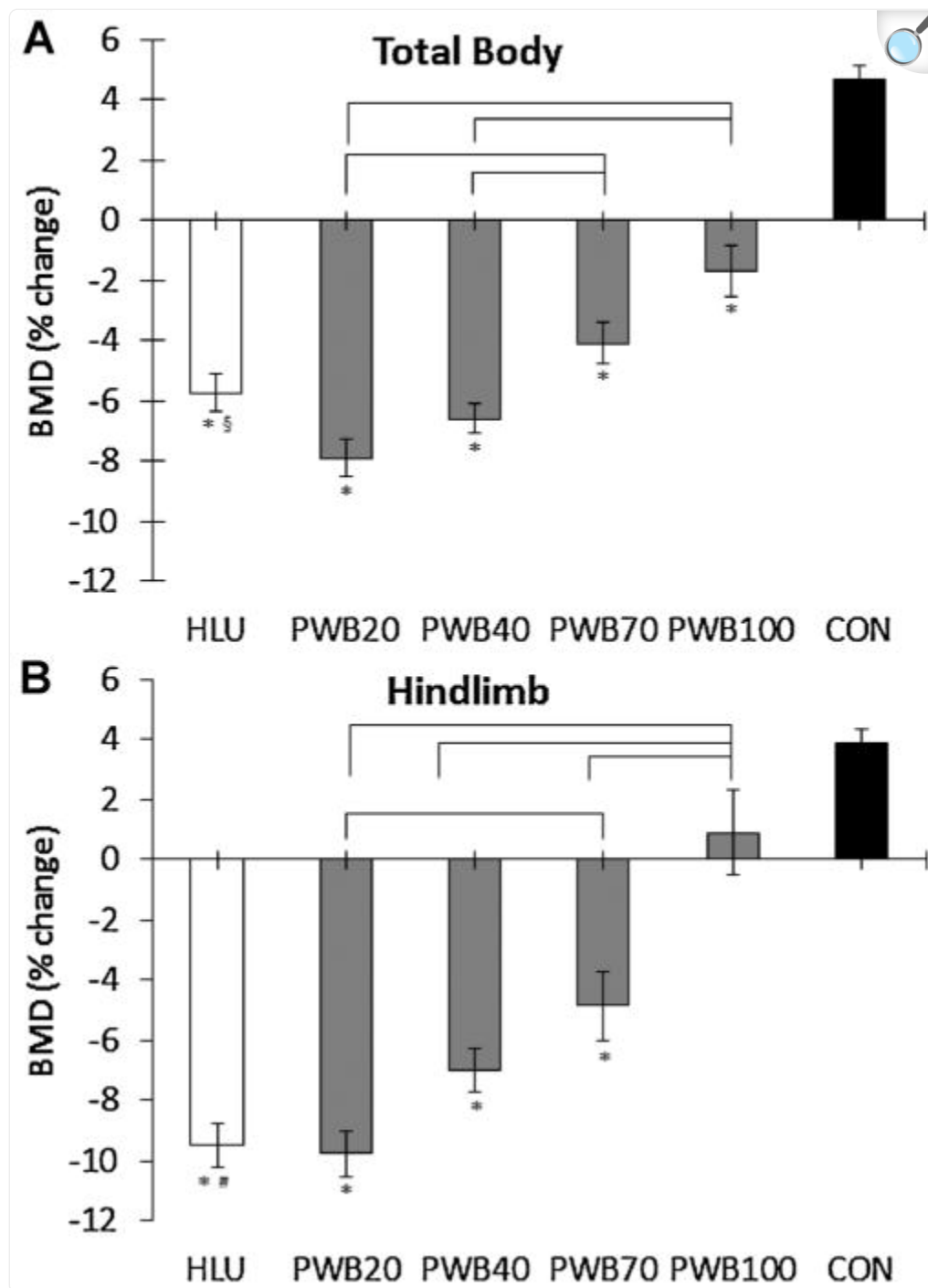
Relationship between weight bearing and the changes in bone and muscle outcomes after 21 days of partial weight bearing at 20%, 40%, 70%, or 100% of body weight. (A) Soleus and gastrocnemius muscle mass normalized by body mass. (B) Bone mineral density (BMD) of the total body and hindlimb. (C) Trabecular bone volume fraction (BV/TV) and thickness of the distal femur. (D) Cortical area and thickness of the femur midshaft. Equations of the best fit line are displayed for linear regressions that were significant and residuals were normally distributed with equal variance over the range of expected values.

The PWS harness itself had minimal effects on muscle mass, because soleus wet weight was similar in the PWB100 and CON groups, though gastrocnemius wet weight was slightly lower in PWB100 versus CON ( $-3.3\%$ ,  $p=0.03$ ).

## BMD

Total body and hindlimb BMD were comparable among all groups at baseline. Total body BMD increased in CON mice ( $4.7\% \pm 2.8\%$  versus baseline;  $p < 0.0001$ ), whereas PWB100 controls did not change significantly from baseline ( $-1.7\% \pm 2.7\%$ ,  $p = 0.08$  versus baseline;  $p < 0.001$  versus CON). Unloading, either by PWB or HLU, led to declines in BMD that were different from CON ([Fig. 5](#)). Further, within the PWB groups, the declines in total body BMD were linearly related to weightbearing, with a  $0.78\% \pm 0.1\%$  decrease in BMD for every 10% decrease in percent weight bearing ( $p < 0.0001$ ,  $R^2 = 0.42$ ; [Figs. 4B, 5A](#)). Similar patterns, but greater in magnitude, were seen for the leg region, with a  $1.2\% \pm 0.2\%$  decrease in hindlimb BMD for every 10% decrease in weight bearing ( $p < 0.0001$ ,  $R^2 = 0.42$ ; [Figs. 4B, 5B](#)). BMD declined less in HLU than PWB20 for the total body ( $-5.7\% \pm 3.0\%$  versus  $-7.9\% \pm 2.7\%$ ,  $p = 0.02$ ), but declined similarly at the hindlimb ([Fig. 5B](#)).

Fig. 5.



[Open in a new tab](#)

Percent change in (A) total body and (B) hindlimb bone mineral density from baseline to day 21 (mean  $\pm$  SEM). \* =Different from CON ( $p < 0.05$ ), § =HLU different from PWB20, PWB100 ( $p < 0.05$ ), # =HLU different from PWB70, PWB100 ( $p < 0.05$ ), brackets =pairwise differences between PWB groups (ANOVA



with Scheffé post hoc,  $p < 0.05$ ).

Of note, there was a strong correlation ( $r = 0.75$ ) between gastrocnemius mass and percent change in hindlimb BMD of all groups.

## Bone microarchitecture

The PWS harness alone had no influence on trabecular bone volume or microarchitecture; however, a few cortical bone parameters were slightly lower in PWB100 compared to CON, including femoral midshaft and metaphyseal cortical thicknesses ( $-7\%$  to  $-8\%$ ; [Table 2](#)).

Table 2.

Effect of HLU and PWB on Cortical and Trabecular Bone Microarchitecture at Distal Femur and Femoral Midshaft

	HLU ( <i>n</i> =23)	PWB20 ( <i>n</i> =19)	PWB40 ( <i>n</i> =21)	PWB70 ( <i>n</i> =18)	PWB100 ( <i>n</i> =10)	CON ( <i>n</i> =37)
Trabecular						
BV/TV (%)	8.00 ± 1.9 <sub>a</sub>	7.27 ± 1.6 <sub>a, b, c</sub>	8.57 ± 1.3 <sub>a</sub>	8.88 ± 1.9 <sub>a</sub>	9.94 ± 2.0	10.31 ± 1.4
Tb.N (1/mm)	3.72 ± 0.23	3.62 ± 0.24 <sub>a</sub>	3.76 ± 0.22	3.68 ± 0.26 <sub>a</sub>	3.76 ± 0.30	3.86 ± 0.14
Tb.Th (µm)	47.2 ± 2.9 <sub>a</sub>	47.2 ± 3.0 <sub>a, b</sub>	48.9 ± 3.2 <sub>a, b</sub>	49.5 ± 3.7 <sub>a, b</sub>	53.5 ± 1.3	53.1 ± 2.5
SMI	3.03 ± 0.20 <sub>d</sub>	3.23 ± 0.20 <sub>a</sub>	3.07 ± 0.14	3.05 ± 0.22	3.05 ± 0.23	2.97 ± 0.21
DA	1.25 ± 0.06 <sub>a</sub>	1.24 ± 0.05 <sub>a, b, c</sub>	1.27 ± 0.05 <sub>a</sub>	1.29 ± 0.05	1.31 ± 0.07	1.32 ± 0.05
Cortical						
Diaphysis						
Ct.Th (µm)	134 ± 6 <sub>a</sub>	131 ± 5 <sub>a, b</sub>	137 ± 9 <sub>a, b</sub>	137 ± 9 <sub>a, b</sub>	149 ± 14 <sub>a</sub>	161 ± 8
Tt.Ar (mm <sup>2</sup> )	1.56 ± 0.10	1.55 ± 0.08	1.54 ± 0.10	1.59 ± 0.06	1.59 ± 0.08	1.57 ± 0.07
Ct.Ar (mm <sup>2</sup> )	0.55 ± 0.03 <sub>a</sub>	0.54 ± 0.03 <sub>a, b</sub>	0.56 ± 0.04 <sub>a, b</sub>	0.57 ± 0.04 <sub>a, b</sub>	0.61 ± 0.05 <sub>a</sub>	0.66 ± 0.03
Ct.Ar/Tt.Ar (%)	35.5 ± 1.6 <sub>a</sub>	34.8 ± 1.1 <sub>a, b</sub>	36.2 ± 2.2 <sub>a, b</sub>	35.7 ± 1.9 <sub>a, b</sub>	38.6 ± 3.0 <sub>a</sub>	41.7 ± 1.7
<i>J</i> (mm <sup>4</sup> )	0.24 ± 0.03 <sub>a</sub>	0.23 ± 0.03 <sub>a, b</sub>	0.24 ± 0.03 <sub>a, b</sub>	0.25 ± 0.02 <sub>a</sub>	0.27 ± 0.03	0.28 ± 0.02
Metaphysis						
Ct.Th (µm)	98 ± 5 <sub>a, d</sub>	93 ± 4 <sub>a, b</sub>	98 ± 5 <sub>a, b</sub>	98 ± 7 <sub>a, b</sub>	111 ± 9 <sub>a</sub>	121 ± 6
Tt.Ar (mm <sup>2</sup> )	2.51 ± 0.15	2.48 ± 0.12	2.53 ± 0.17	2.57 ± 0.10	2.59 ± 0.12	2.50 ± 0.12
Ct.Ar (mm <sup>2</sup> )	0.57 ± 0.03 <sub>a, d</sub>	0.54 ± 0.04 <sub>a, b</sub>	0.57 ± 0.04 <sub>a, b</sub>	0.57 ± 0.04 <sub>a, b</sub>	0.66 ± 0.06 <sub>a</sub>	0.71 ± 0.05

	HLU ( <i>n</i> =23)	PWB20 ( <i>n</i> =19)	PWB40 ( <i>n</i> =21)	PWB70 ( <i>n</i> =18)	PWB100 ( <i>n</i> =10)	CON ( <i>n</i> =37)
Ct.Ar/Tt.Ar (%)	22.7 ± 1.3 <sup>a,d</sup>	21.6 ± 1.3 <sup>a,b</sup>	22.5 ± 1.7 <sup>a,b</sup>	22.3 ± 1.3 <sup>a,b</sup>	25.5 ± 2.1 <sup>a</sup>	28.5 ± 1.9

[Open in a new tab](#)

Values are mean ± SD.

HLU =hindlimb unloaded; PWB =partial weight bearing; PWB20 =PWB at 20% of body mass; PWB40 =at 40% of body mass; PWB70 =at 70% of body mass; PWB100 =at 100% of body mass; CON =control; BV/TV =bone volume/total volume; Tb.N =trabecular number; Tb.Th =trabecular thickness; SMI =structure model index; DA =degree of anisotropy; Ct.Th =cortical thickness; Tt.Ar =total cross-sectional area; Ct.Ar =cortical bone area; Ct.Ar/Tt.Ar =cortical area fraction; *J* =polar moment of inertia.

<sup>a</sup>Different from CON by ANOVA among all groups, Dunnett's post hoc test ( $p < 0.05$ ).

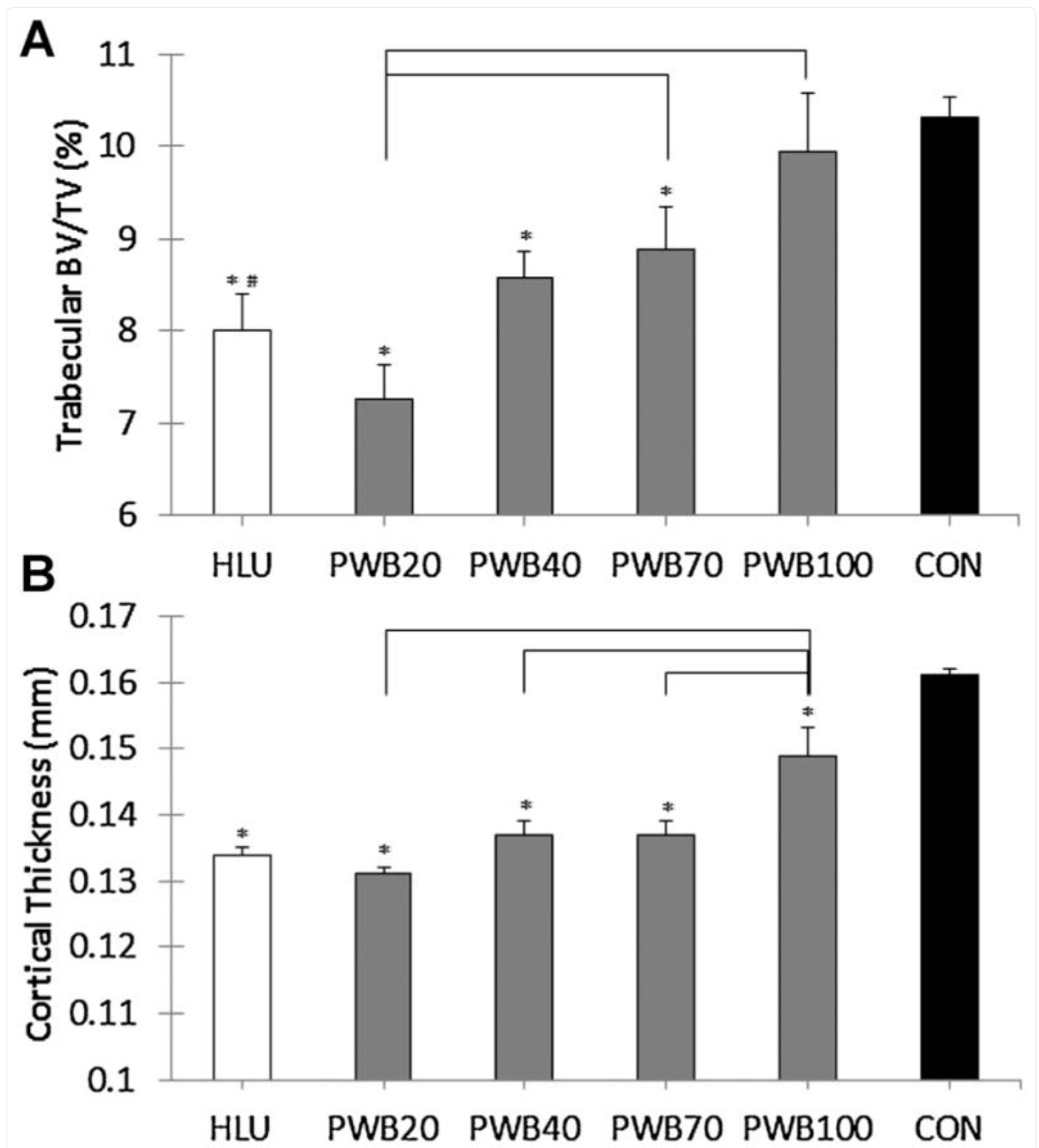
<sup>b</sup>Different from PWB100 by ANOVA among 4 PWB levels, Scheffé post hoc test ( $p < 0.05$ ).

<sup>c</sup>Different from PWB70 by ANOVA among 4 PWB levels, Scheffé post hoc test ( $p < 0.05$ ).

<sup>d</sup>Difference between HLU and PWB20 ( $p < 0.05$ ) by *t* test.

As was seen with BMD, in the PWB groups, trabecular bone volume and microarchitecture at the distal femur tended to deteriorate in proportion to the degree of unloading, such that Tb.BV/TV was 27% lower in PWB20 than PWB100 (Table 2, Fig. 6A). Indeed, distal femur Tb.BV/TV was linearly associated with weight-bearing level ( $R^2 = 0.20$ ,  $p < 0.0001$ ; Fig. 4C). Specific microarchitectural changes associated with unloading included trabecular thinning resulting in more rod-like, less-aligned trabeculae. With regard to cortical bone morphology, unloading did not impact total bone cross-sectional area, but did lead to significantly lower cortical bone area (−18% to −24%) and a thinner cortex (−15% to −23%) at both the femoral mid-diaphysis and distal metaphyseal regions compared to PWB100 (Table 2, Fig. 6B). Partial unloading also led to significant reduction in polar moment of inertia compared to CON. Cortical area of the femoral midshaft was linearly associated with weight bearing ( $R^2 = 0.24$ ,  $p < 0.0001$ ; Fig. 4D).

Fig. 6.



[Open in a new tab](#)

Femur microarchitectural measurements of (A) trabecular bone volume fraction at the distal metaphysis and (B) cortical thickness of the mid-diaphysis (mean  $\pm$  SEM). \* =Different from CON ( $p < 0.05$ ), # =HLU different from PWB100 ( $p < 0.05$ ), brackets =pairwise differences between PWB groups (ANOVA with Scheffé post hoc,  $p < 0.05$ ).

Mice exposed to HLU had significantly worse bone microarchitecture compared to CON, but either similar or slightly better trabecular and cortical bone morphology compared to PWB20 ([Table 2](#), [Fig. 6](#)). For example, at the distal femoral metaphysis, HLU mice had higher Ct.Th, Ct.Ar, and Ct.Ar/Tt.Ar and more plate-like trabecular structure than PWB20 ( $p < 0.008$ ).

## Femoral bone strength

Femoral bone biomechanical properties were similar in CON and PWB100 ([Table 3](#)). Maximum force (−19% to −21%) and stiffness (−14% to −20%) were lower in all partially and fully unloaded groups relative to CON ( $p < 0.0001$  versus CON; [Table 3](#)), but comparable to each other. Estimated elastic modulus did not differ among all groups.

Table 3.

Effect of Unloading on Femoral Diaphysis Three-Point Bend Testing

	HLU	PWB20	PWB40	PWB70	PWB100	CON
Stiffness (N/mm)	43.1 ± 6.4 <sup>a</sup> <sub>—</sub>	46.0 ± 4.1 <sup>a b</sup> <sub>—, —</sub>	43.0 ± 6.4 <sup>a b</sup> <sub>—, —</sub>	44.3 ± 6.6 <sup>a b</sup> <sub>—, —</sub>	53.9 ± 7.8	53.5 ± 7.0
Maximum force (N)	9.5 ± 0.9 <sup>a</sup> <sub>—</sub>	9.6 ± 0.8 <sup>a b</sup> <sub>—, —</sub>	9.8 ± 0.9 <sup>a b</sup> <sub>—, —</sub>	9.8 ± 0.9 <sup>a b</sup> <sub>—, —</sub>	11.5 ± 1.0	12.1 ± 1.0
Estimated Young's modulus (GPa)	7.9 ± 2.0	9.2 ± 3.1	7.9 ± 1.8	9.5 ± 2.3	8.4 ± 2.2	8.7 ± 2.6

[Open in a new tab](#)

Values are mean ± SD.

HLU =hindlimb unloaded; PWB =partial weight bearing; PWB20 =PWB at 20% of body mass; PWB40 =PWB at 40% of body mass; PWB70 =PWB at 70% of body mass; PWB100 =PWB at 100% of body mass; CON =control.

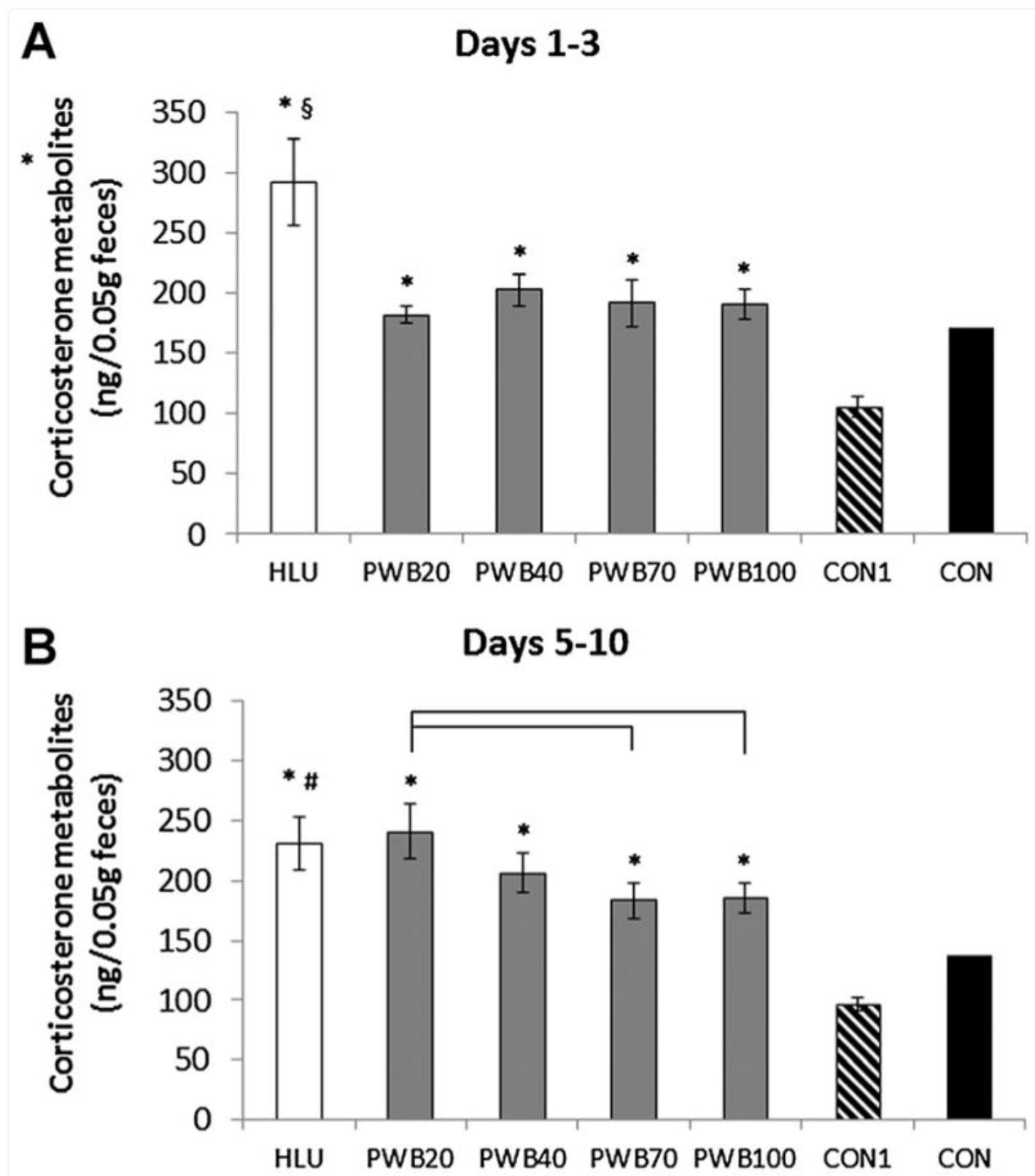
<sup>a</sup>Different from CON by ANOVA among all groups, Dunnett post hoc test ( $p < 0.05$ ).

<sup>b</sup>Different from PWB100 by ANOVA of 4 PWB levels, Scheffé post hoc test ( $p < 0.05$ ).

## Effects of PWB on adrenocortical activity

All groups had the same baseline level of fecal corticosterone metabolites (FCM). CON1, the mice singly housed in standard cages, had the lowest FCM levels for the duration of the experiment though we could not determine if this was significantly less than the group-housed CON due to the single CON measurement at each time point ([Fig. 7](#)). All HLU and PWB groups had higher FCM levels than CON1 throughout the study ( $p < 0.05$ ). Further, for days 1 to 3, FCM levels in HLU were higher than all PWB groups ( $p < 0.05$ ). For days 5 to 10, FCM levels in HLU decreased to the same level as those in PWB20, PWB40, and PWB100, but remained significantly higher than PWB70 ( $p < 0.05$ ). All PWB groups had the same measured FCM levels for both time blocks, except concentrations in PWB20 were higher than PWB70 and PWB100 on days 5 to 10 ( $p < 0.05$ ).

Fig. 7.



Mean  $\pm$  SEM concentrations of fecal corticosterone metabolites from (A) days 1 to 3 and (B) days 5 to 10. \* =Different from CON1 ( $p < 0.05$ ); brackets =pairwise differences between PWB groups ( $p < 0.05$ ); § =HLU different from PWB20, PWB40, PWB70, PWB100; # =HLU different from PWB70.

## Discussion

---

We investigated the influence of reduced weight bearing on the musculoskeletal system by comparing the bone and muscle adaptation to three levels of PWB with that of HLU and fully weight-bearing controls. We hypothesized that PWB would differentially attenuate muscle atrophy and bone loss as compared to full unloading, and more specifically, that there would be a linear relationship between the percent of weight bearing and degree of bone and muscle loss. Further, we hypothesized that the PWS apparatus itself would have no effect on bone and muscle tissue or gait kinematics.

Within the PWB groups, we found a strong dependence of most bone and muscle outcomes on the degree of PWB. Of the variables that were influenced by loading, all decreased monotonically with decreasing weight bearing. Further, calf muscle mass, total body and hindlimb bone mineral density, femoral trabecular bone volume, and cortical bone area met statistical criteria to be linearly related to weightbearing. For the longitudinal measurements (total body and hindlimb BMD) approximately 40% of the variation in bone loss was explained by the level of PWB. Although highly significant, the PWB level explained less of the variation in bone and muscle parameters measured at the end of the study, likely reflecting the interanimal variation at baseline not accounted for by end of study measures. It is not surprising that the PWB level did not explain more of the variation in bone and muscle loss given the rough measure of bone loading that is provided by the static ground reaction forces (eg, PWB level). The variation in bone and muscle outcomes at each weight-bearing level are likely due to the heterogeneous loading experienced by the mice because activity level, and therefore number of strain cycles and total strain stimulus, could not be controlled.

We addressed whether the PWS harness alone influenced musculoskeletal outcomes. Whereas most outcomes did not differ between group-housed controls and mice harnessed in the suspension rig but fully loaded to 100% of their body weight, there were minor differences in some parameters. These differences were not observed previously when we used a jacketed, but not harnessed, control.<sup>(10)</sup> It is possible that the changes we found were brought about by experimental conditions causing disturbances in stress because harnessed mice had higher stress levels than singly-housed mice, but maintained total body mass consistent with the controls. Also, there are other mechanical factors that may have contributed to these observations. First, gait is slightly modified by the addition of a harness, which could alter the mechanical environment of the hindlimb. The gait alterations at 100% weight bearing were minimal, with only a slight increase in stance width during harnessed locomotion relative to control animals. Second, the harness, although providing 100% loading as measured during static weight bearing on a scale, could have affected the animals' overall physical activity leading to a decrease in total dynamic loading. Third, whenever the animal ventured away from the



central axis of the cage, thus stretching the harness, the restoring force of the spring would partially unload the animal relative to its distance from the center. A low spring constant was chosen to minimize this restoring force, estimated to be a maximum of 32% of body weight in the vertical direction at the furthest edge of the cage. Taken altogether, there may have been a systemic or mechanical unloading effect of the harness in the fully weight-bearing control group and results should be interpreted with this in mind. Still, only a few bone and muscle outcomes were altered with the harness and any differences between PWB100 and CON were greatly exceeded by the impact of reduced weight bearing.

Comparison of PWB to HLU led to several interesting observations. Muscle atrophy was greater in HLU than PWB20, as expected. However, contrary to our initial hypothesis, hindlimb BMD and microarchitecture of tail suspended animals fared as well or better than those of mice bearing 20% of their body weight. This result was unexpected based on the paradigm that mechanical loading provides the primary stimulus for musculoskeletal maintenance, the high correlation between muscle and bone measures, and the assumption that mechanical loading is less for HLU mice than PWB20. One possible explanation is that HLU mice were not truly loaded less than PWB20, because the unloaded hindlimb continued to receive stimulation through muscular contractions acting against limb inertia. Future studies should measure strain in the hindlimb during HLU and PWB to verify that strain decreases as predicted.

Yet it is paradoxical that HLU mice experienced greater muscle atrophy but maintained higher bone mass than PWB20. This discrepancy between relative changes in bone and muscle evokes an alternative explanation that systemic factors influenced the muscle/bone interactions. Possible systemic factors that may play a role include elevated corticosterone levels and cephalad fluid shift. High glucocorticoid levels are catabolic to both bone and muscle. Based on our measurements of fecal corticosterone metabolites, both PWB20 and HLU groups had elevated adrenocortical activity throughout the experiment, but stress was higher in HLU for the first 3 days and thus is not consistent with lesser bone loss seen in HLU. Cephalad fluid shift is induced by HLU due to the approximately 30-degree head-down tilt, but is not duplicated by PWS. It has been proposed that this fluid shift leads to increased perfusion of the cephalically located skeleton, providing an osteogenic stimulus,<sup>(21,22)</sup> which may cause the release of anti-catabolic factors systemically. Although speculative, this in turn might offset the skeletal effects of unloading in the hindlimbs while not affecting muscle. Ultimately, we lack a suitable explanation for the discrepant muscle and bone changes with HLU. However, it is certain that hindlimb unloading is not equivalent to 0% PWB; and that the PWB and HLU models are functionally different.

The PWS model is well suited to test the tenets proposed in the mechanostat theory. Specifically, the theory asserts the existence of a “lazy zone” in which bone mass does not change over a wide range of normal strain, bounded by a lower threshold of minimum effective strain at 50 to 200  $\mu\epsilon$  and an upper threshold of 2000 to 3000  $\mu\epsilon$ .<sup>2</sup> Therefore, a conservative estimate of the width of the lazy zone is 200 to 2000  $\mu\epsilon$ , or in other terms, 18% to 182% of the median strain. However, we saw definitive reductions in bone mass, architecture, and strength with a decrease in weight bearing by as little as 30% (ie, PWB70). For bone remodeling to have occurred, the lower threshold must be higher than 70% of normal weight bearing. Thus the data support a physiologic window of normal strain stimulus (lazy zone) much

narrower on the underloading side than that proposed by Frost.<sup>(1,2)</sup> Furthermore, if it were assumed that the bone changes identified in the skeletons of PWB100 animals resulted from minor reductions in loading, then the lower strain threshold would have to exist very close to normal weight-bearing strain. This is consistent with Lanyon's hypothesis of bone adaptation<sup>(23,24)</sup> and is supported by a recent study in which sciatic neurectomized mice received axial loading to different peak loads and resultant bone mass/strength measures were linearly related to peak load, with no evidence of a lazy zone.<sup>(25)</sup> If this theory were true, extended minor reductions in physical activity would be suggested to cause proportionate degrees of bone loss. Although bed rest has clearly been shown to reduce bone mass, periods of relatively reduced activity, such as that which may occur during hospitalization<sup>(26)</sup> or winter months,<sup>(27)</sup> should also be considered as risks to bone health. Then again, it is possible that factors other than strain may have led to slight changes in select outcomes. Further studies should quantify the reduction in loading from PWS harnessing at 100% weight bearing and less to determine the strain threshold below which bone resorption is initiated.

The maintenance of normal bone loading patterns, through preserved quadrupedal gait kinematics, with a reduction in magnitude, through PWB, is an important advantage of this PWB model. In other models that use external loading to modify the mechanical environment, there is a mismatch in strain distribution between normal loading and experimentally applied loading, which often leads to regional variability in effects on bone and complicates interpretation.<sup>(25,28,29)</sup> The expected preserved strain distribution in this model resolves the problem of not knowing how the experimental loading differs from normal. Thereby, PWB could be a powerful tool in discriminating regional differences in bone's sensitivity to mechanical signals.

This study has several limitations. The PWS harness could be improved by the use of a dual-axis rig that would allow the mouse to move around all areas of the cage with a constant unweighting force. Second, because it is putatively mechanical strain to which bone responds, it would be important to quantify the strains engendered at varying weight-bearing levels to relate bone adaptive changes reported here to alterations in the local mechanical environment. Finally, we investigated only one time point, and future studies involving multiple time points are needed to explore the time-dependence of musculoskeletal adaptation. Despite these limitations, we showed that the PWS model is highly effective in applying controllable, reduced, long-term loading that produces predictable, discrete adaptive changes in muscle and bone of the hindlimb. This is the first study with the PWS model to include a concurrent HLU group, allowing for comparison to an established model of disuse-induced loss, and a PWB100 control group, to account for the independent effect of the PWS harness. Finally, we demonstrated that the PWS system is less stressful than HLU by measuring fecal corticosterone metabolites.

In conclusion, this study used a partial unloading model that largely preserves normal gait to demonstrate that bone and muscle loss are linearly related to the degree of unloading, as measured by static weight bearing. Using this tunable model we were able to thoroughly describe bone and muscle adaptation for loading magnitudes in the spectrum between total unloading and normal mechanical loading for the first time, and found that even a load reduction to 70% of normal weight bearing was associated with significant bone deterioration and muscle atrophy. The PWB model will be useful

for future studies investigating the specific local mechanical signals, systemic hormones, and molecular mechanisms that contribute to disuse-induced bone loss and muscle atrophy.

## Acknowledgments

---

This work was supported by NIH R21 AR057522, NASA NNX10AE39G, and the National Space Biomedical Research Institute through NASA NCC 9-58. RE was supported by a NASA-Jenkins predoctoral fellowship. JMS was supported by a Northrop Grumman Aerospace Systems Ph.D. Training Fellowship. We thank Erika Wagner for consultation on the use of the PWS system. We thank Timothy O'Shea for his assistance with the processing of fecal samples.

## Footnotes

---

### Disclosures

All authors state that they have no conflicts of interest.

Authors' roles: RE: study design and conduct; data collection, analysis and interpretation; manuscript drafting, revision, and approval. JMS: study design and conduct; data collection and analysis; manuscript approval. AMC: study conduct, data collection and analysis; manuscript revision and approval. RP: corticosterone EIA; manuscript approval. BAC: study design, conduct of gait kinematics substudy; manuscript revision and approval. MLB: study design; data analysis and interpretation; manuscript drafting, revision, and approval. RE takes responsibility for the integrity of the data analysis.

## References

---

1. Frost HM. Perspectives: a proposed general model of the “mechanostat” (suggestions from a new skeletal-biologic paradigm) *Anat Rec.* 1996;244(2):139–47. doi: 10.1002/(SICI)1097-0185(199602)244:2<139::AID-AR1>3.0.CO;2-X. [[DOI](#)] [[PubMed](#)] [[Google Scholar](#)]
2. Frost HM. Bone “mass” and the “mechanostat”: a proposal. *Anat Rec.* 1987;219(1):1–9. doi: 10.1002/ar.1092190104. [[DOI](#)] [[PubMed](#)] [[Google Scholar](#)]
3. Robling AG, Castillo AB, Turner CH. Biomechanical and molecular regulation of bone remodeling. *Annu Rev Biomed Eng.* 2006;8:455–98. doi: 10.1146/annurev.bioeng.8.061505.095721. [[DOI](#)] [[PubMed](#)] [[Google Scholar](#)]

4. Morey-Holton E, Globus RK, Kaplansky A, Durnova G. The hindlimb unloading rat model: Literature overview, technique update and comparison with space flight data. *Adv Space Biol Med.* 2005;10:7–40. doi: 10.1016/s1569-2574(05)10002-1. [[DOI](#)] [[PubMed](#)] [[Google Scholar](#)]
5. Tuukkanen J, Wallmark B, Jalovaara P, Takala T, Sjögren S, Väänänen K. Changes induced in growing rat bone by immobilization and remobilization. *Bone.* 1991 Jan 1;12(2):113–8. doi: 10.1016/8756-3282(91)90009-8. [[DOI](#)] [[PubMed](#)] [[Google Scholar](#)]
6. Thompson DD, Rodan GA. Indomethacin inhibition of tenotomy-induced bone resorption in rats. *J Bone Miner Res.* 1988 Aug 1;3(4):409–14. doi: 10.1002/jbmr.5650030407. [[DOI](#)] [[PubMed](#)] [[Google Scholar](#)]
7. Földes I, Gyarmati J, Rapcsák M, Szöör A, Szilágyi T. Effect of plaster-cast immobilization on the bone. *Acta Physiol Hung.* 1986 Jan 1;67(4):413–8. [[PubMed](#)] [[Google Scholar](#)]
8. Warner SE, Sanford DA, Becker BA, Bain SD, Srinivasan S, Gross TS. Botox induced muscle paralysis rapidly degrades bone. *Bone.* 2006 Feb;38(2):257–64. doi: 10.1016/j.bone.2005.08.009. [[DOI](#)] [[PMC free article](#)] [[PubMed](#)] [[Google Scholar](#)]
9. National Research Council of the National Academies. Committee for the Decadal Survey on Biological and Physical Sciences in Space, Space Studies Board, Aeronautics and Space Engineering Board, and Division on Engineering and Physical Sciences. Recapturing a future for space exploration: life and physical sciences research for a new era. Washington, DC: National Academies Press; 2011. [[Google Scholar](#)]
10. Wagner EB, Granzella NP, Saito H, Newman DJ, Young LR, Bouxsein ML. Partial weight suspension: a novel murine model for investigating adaptation to reduced musculoskeletal loading. *J Appl Physiol.* 2010 Aug;109(2):350–7. doi: 10.1152/japplphysiol.00014.2009. [[DOI](#)] [[PMC free article](#)] [[PubMed](#)] [[Google Scholar](#)]
11. Morey-Holton ER, Globus RK. Hindlimb unloading rodent model: technical aspects. *J Appl Physiol.* 2002 Apr 1;92(4):1367–77. doi: 10.1152/japplphysiol.00969.2001. [[DOI](#)] [[PubMed](#)] [[Google Scholar](#)]
12. Vincelette J, Xu Y, Zhang LN, Schaefer CJ, Vergona R, Sullivan ME, Hampton TG, Wang YX. Gait analysis in a murine model of collagen-induced arthritis. *Arthritis Res Ther.* 2007;9(6):R123. doi: 10.1186/ar2331. [[DOI](#)] [[PMC free article](#)] [[PubMed](#)] [[Google Scholar](#)]
13. Bouxsein ML, Boyd SK, Christiansen BA, Guldberg RE, Jepsen KJ, Müller R. Guidelines for assessment of bone microstructure in rodents using micro-computed tomography. *J Bone Miner Res.* 2010;25(7):1468–86. doi: 10.1002/jbmr.141. [[DOI](#)] [[PubMed](#)] [[Google Scholar](#)]
14. Glatt V, Canalis E, Stadmeier L, Bouxsein ML. Age-related changes in trabecular architecture differ in female and male C57BL/6J mice. *J Bone Miner Res.* 2007 Aug 1;22(8):1197–207. doi: 10.1359/jbmr.070507.

[\[DOI\]](#) ] [\[PubMed\]](#) [\[Google Scholar\]](#) ]

15. Hildebrand T, Ruegsegger P. Quantification of bone microarchitecture with the structure model index. *Comput Methods Biomech Biomed Engin.* 1997;1(1):15–23. doi: 10.1080/01495739708936692. [\[DOI\]](#) ] [\[PubMed\]](#) [\[Google Scholar\]](#) ]

16. Hildebrand T, R  gsegger P. A new method for the model-independent assessment of thickness in three-dimensional images. *J Microsc.* 1997;185(1):67–75. [\[Google Scholar\]](#) ]

17. Hildebrand T, Laib A, M  ller R, Dequeker J, R  gsegger P. Direct three-dimensional morphometric analysis of human cancellous bone: microstructural data from spine, femur, iliac crest, and calcaneus. *J Bone Miner Res.* 1999;14(7):1167–74. doi: 10.1359/jbmr.1999.14.7.1167. [\[DOI\]](#) ] [\[PubMed\]](#) [\[Google Scholar\]](#) ]

18. Brodt MD, Ellis CB, Silva MJ. Growing C57Bl/6 mice increase whole bone mechanical properties by increasing geometric and material properties. *J Bone Miner Res.* 1999;14(12):2159–66. doi: 10.1359/jbmr.1999.14.12.2159. [\[DOI\]](#) ] [\[PubMed\]](#) [\[Google Scholar\]](#) ]

19. Touma C, Sachser N, M  stl E, Palme R. Effects of sex and time of day on metabolism and excretion of corticosterone in urine and feces of mice. *Gen Comp Endocrinol.* 2003 Feb 15;130(3):267–78. doi: 10.1016/s0016-6480(02)00620-2. [\[DOI\]](#) ] [\[PubMed\]](#) [\[Google Scholar\]](#) ]

20. Touma C, Palme R, Sachser N. Analyzing corticosterone metabolites in fecal samples of mice: a noninvasive technique to monitor stress hormones. *Horm Behav.* 2004 Jan;45(1):10–22. doi: 10.1016/j.yhbeh.2003.07.002. [\[DOI\]](#) ] [\[PubMed\]](#) [\[Google Scholar\]](#) ]

21. Colleran PN, Wilkerson MK, Bloomfield SA, Suva LJ, Turner RT, Delp MD. Alterations in skeletal perfusion with simulated microgravity: a possible mechanism for bone remodeling. *J Appl Physiol.* 2000 Sep;89(3):1046–54. doi: 10.1152/jappl.2000.89.3.1046. [\[DOI\]](#) ] [\[PubMed\]](#) [\[Google Scholar\]](#) ]

22. Turner CH, Forwood MR, Otter MW. Mechanotransduction in bone: do bone cells act as sensors of fluid flow? *FASEB J.* 1994 Aug 1;8(11):875–8. doi: 10.1096/fasebj.8.11.8070637. [\[DOI\]](#) ] [\[PubMed\]](#) [\[Google Scholar\]](#) ]

23. Rubin C, Lanyon L. Regulation of bone mass by mechanical strain magnitude. *Calcif Tissue Int.* 1985 Jul 1;37(4):411–7. doi: 10.1007/BF02553711. [\[DOI\]](#) ] [\[PubMed\]](#) [\[Google Scholar\]](#) ]

24. Lanyon LE. Functional strain in bone tissue as an objective, and controlling stimulus for adaptive bone remodelling. *J Biomech.* 1987;20(11–12):1083–93. doi: 10.1016/0021-9290(87)90026-1. [\[DOI\]](#) ] [\[PubMed\]](#) [\[Google Scholar\]](#) ]

25. Sugiyama T, Meakin LB, Browne WJ, Galea GL, Price JS, Lanyon LE. Bones’ adaptive response to

mechanical loading is essentially linear between the low strains associated with disuse and the high strains associated with the lamellar/woven bone transition. *J Bone Miner Res.* 2012 Aug;27(8):1784–93. doi: 10.1002/jbmr.1599. [[DOI](#)] [[PMC free article](#)] [[PubMed](#)] [[Google Scholar](#)]

26. Krolner B, Toft B. Vertebral bone loss: An unheeded side effect of therapeutic bed rest. *Clin Sci (Lond)* 1983 May;64(5):537–40. doi: 10.1042/cs0640537. [[DOI](#)] [[PubMed](#)] [[Google Scholar](#)]

27. Bergstralh EJ, Sinaki M, Offord KP, Wahner HW, Melton LJ., 3rd Effect of season on physical activity score, back extensor muscle strength, and lumbar bone mineral density. *J Bone Miner Res.* 1990 Apr;5(4):371–7. doi: 10.1002/jbmr.5650050410. [[DOI](#)] [[PubMed](#)] [[Google Scholar](#)]

28. Mosley JR, March BM, Lynch J, Lanyon LE. Strain magnitude related changes in whole bone architecture in growing rats. *Bone.* 1997 Mar;20(3):191–8. doi: 10.1016/s8756-3282(96)00385-7. [[DOI](#)] [[PubMed](#)] [[Google Scholar](#)]

29. Mosley JR, Lanyon LE. Strain rate as a controlling influence on adaptive modeling in response to dynamic loading of the ulna in growing male rats. *Bone.* 1998 Oct;23(4):313–8. doi: 10.1016/s8756-3282(98)00113-6. [[DOI](#)] [[PubMed](#)] [[Google Scholar](#)]